| OF |

AD
AO74275

END
DATE
FILMED
-10-79
DDC

1.0

4.5
5.0
5.6
6.3

2.8

2.5

3.2

2.2

3.6

4.0

2.0

1.1

1.8

1.25

1.4

1.6

MICROCOPY RESOLUTION TEST CHART

NATIONAL BUREAU OF STANDARDS-1963-A

LEVEL

# MODELING THE REFRACTIVE INDEX STRUCTURE PARAMETER IN THE MARINE PLANETARY BOUNDARY LAYER

Stephen D. Burk, Andreas K. Goroch, and Alan I. Weinstein
Naval Environmental Prediction Research Facility
Monterey, CA

and

Hans A. Panofsky
Meteorology Department
Pennsylvania State University
University Park, PA

**JUNE 1979**

DDC

SEP 26 1979

A

79 09 24 075

14 NEPRF-TR-79-03     10     Stephen D. /Burk, Andreas K. /Goroch
Alan I. /Weinstein   Hans A. /Panofsky

| REPORT DOCUMENTATION PAGE | READ INSTRUCTIONS BEFORE COMPLETING FORM |
|---|---|
| 1 REPORT NUMBER NAVENVPREDRSCHFAC Technical Report TR 79-03 | 2. GOVT ACCESSION NO. | 3. RECIPIENT'S CATALOG NUMBER |

| 4. TITLE (and Subtitle) Modeling the Refractive Index Structure Parameter in the Marine Planetary Boundary Layer. | 5. TYPE OF REPORT & PERIOD COVERED Final rept. |
|---|---|
| | 6. PERFORMING ORG. REPORT NUMBER |
| 7. AUTHOR(s) S. Burk, A. Goroch, A. Weinstein, NAVENVPREDRSCHFAC; H. Panofsky, Pennsylvania State University | 8. CONTRACT OR GRANT NUMBER(s) 12 58 p. |
| 9. PERFORMING ORGANIZATION NAME AND ADDRESS Naval Environmental Prediction Research Facility, Monterey, CA 93940 | 10. PROGRAM ELEMENT, PROJECT, TASK AREA & WORK UNIT NUMBERS PE 63754N PN S0182-AA WU 6.3-12 |
| 11. CONTROLLING OFFICE NAME AND ADDRESS Naval Sea Systems Command Department of the Navy Washington, DC 20361 | 12. REPORT DATE June 1979 |
| | 13. NUMBER OF PAGES 58 |
| 14. MONITORING AGENCY NAME & ADDRESS(if different from Controlling Office) | 15. SECURITY CLASS. (of this report) UNCLASSIFIED |
| | 15a. DECLASSIFICATION/DOWNGRADING SCHEDULE |

16. DISTRIBUTION STATEMENT (of this Report)

Approved for public release; distribution unlimited

17. DISTRIBUTION STATEMENT (of the abstract entered in Block 20, if different from Report)

16 S0182AA

18. SUPPLEMENTARY NOTES

19. KEY WORDS (Continue on reverse side if necessary and identify by block number)
Laser propagation
Turbulence
Refractive index fluctuations
Marine planetary boundary layer
Structure function parameters

$C_n^2$

20. ABSTRACT (Continue on reverse side if necessary and identify by block number)

This report summarizes the proceedings, conclusions and recommendations of a two-day workshop (30-31 Jan 1979) on refractive index structure parameter, $C_n^2$, in the marine planetary boundary layer (MPBL).

Scaling laws are described that are adequate to predict $C_n^2$ in the surface layer to an accuracy of approximately a

DD FORM 1473   EDITION OF 1 NOV 68 IS OBSOLETE
1 JAN 73
S N 0102-014-6601

407279

## 20. ABSTRACT (continued)

factor of two. A stepwise procedure is described to predict $C_n^2$ using these scaling steps.

No generally accepted quantitative scaling laws exist in the upper MPBL. Simple second-moment turbulence models hold the best promise for $C_n^2$ prediction in the upper MPBL at this time. After verification these models can be used by them-selves or to generate upper MPBL scaling laws.

$C_n(2)$

**CONTENTS**

# CONTENTS (continued)

## ACKNOWLEDGMENTS

# 1. MODELING THE REFRACTIVE INDEX STRUCTURE PARAMETER IN THE MARINE PLANETARY BOUNDARY LAYER

## 1.1 INTRODUCTION

At the request and under the sponsorship of the Navy's High Energy Laser (HEL) Program Office, the Naval Environmental Prediction Research Facility (NEPRF) hosted a Workshop on Modeling of Refractive Index Structure Parameter, $C_n^2$, in the Marine Planetary Boundary Layer. Appendices A and B are list of attendees and the agenda at the workshop.

NEPRF proposed a preliminary $C_n^2$ model to serve as a strawman for discussion at the workshop. The model is included as Appendix C. The workshop participants reviewed the components of the preliminary model, and suggested modifications to improve the model.

This document summarizes the modified $C_n^2$ model, and presents a state of the art review of marine planetary boundary layer $C_n^2$ modeling. The document represents the consensus opinion of the workshop participants.

## 1.2 HEL PROBLEM

### 1.2.1 Atmospheric Effects on HEL System Performance

Atmospheric conditions degrade HEL system performance by reducing fluence on target in a variety of ways; aerosols and water vapor absorb energy; aerosols scatter energy out of the beam path; atmospheric turbulence spreads the beam fluence; and atmospheric turbulence also causes the beam to wander off its intended target. Figure 1.1 is a schematic representation of these four effects which are shown separately and sequentially in the figure. In nature, each effect occurs simultaneously along the beam.

The aerosol and water vapor elements of the problem are being considered elsewhere within the Navy R&D community. Consequently, these elements were not addressed at the NEPRF workshop, nor do we consider them in this review.
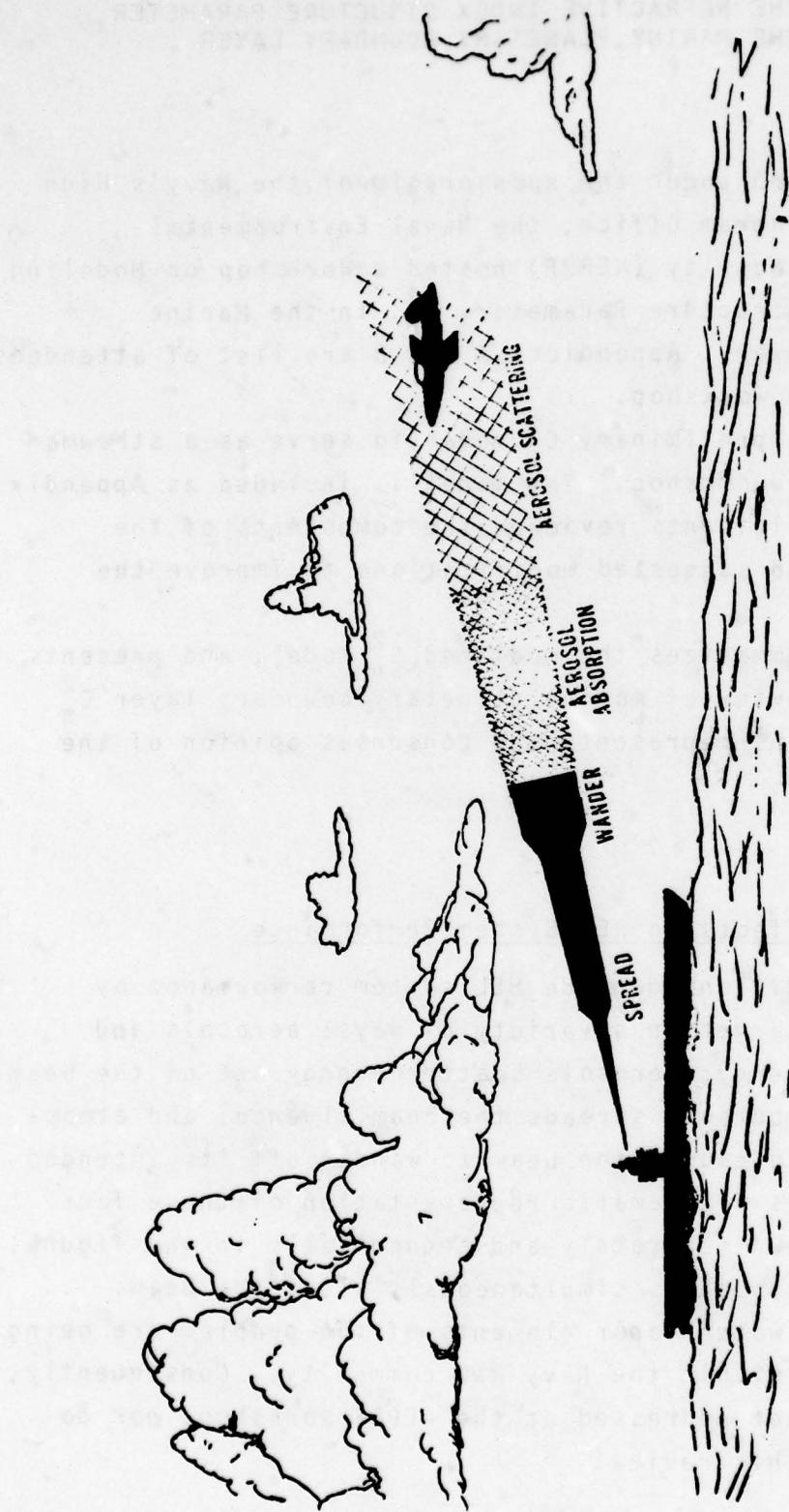
Fig. 1.1 Atmospheric Effects on Laser System Performance. Although the effects are shown here separately and sequentially for purposes of illustration, they can occur together and anywhere along the beam.

## 1.2.2  Turbulence Near the Sea Surface

The Navy is developing laser systems for shipboard operation. From a ship, a laser could be fired horizontally, vertically or at any angle.  In the first case, turbulence near the sea surface degrades the beam.  In the latter two cases, turbulence aloft as well as near the surface can degrade performance.

The degradation of system performance is caused by turbulent fluctuations of refractive index, weighed nonlinearly toward the transmitting end of the propagation path.  Therefore turbulent conditions affect beam quality more when they are near the source than similar conditions near the target.  We call this range dependence.  System performance calculations take range dependence into consideration.

For a surface based laser system, range dependence makes turbulence near the ground degrade system performance more than turbulence aloft.  For this reason and others to be elaborated upon later, we focus upon the atmosphere near the sea surface.  We call this region the marine planetary boundary layer (MPBL) (Fig. 1.2 and 1.3).

## 1.3  TECHNICAL PROBLEM

There are two elements of the technical problem that must be recognized by the reader of this report; (1) the turbulence parameter that is related to HEL system performance is the refractive index structure parameter, $C_n^2$; and (2) $C_n^2$, like many meteorological parameters, behaves differently near the surface, in the MPBL, than it does aloft in the free troposphere.

## 1.3.1  Refractive Index Structure Parameter, $C_n^2$

The structure parameter for any atmospheric variable is a measure of the turbulent fluctuations of that variable over small distances.  For HEL systems, the atmospheric variable of interest is refractive index, and the structure parameter is $C_n^2$.  $C_n^2$ is defined by:

$$C_n^2 = \overline{[n(x+r) - n(x)]^2} \; r^{-2/3} \tag{1.1}$$

3

HEIGHT
Z
15 KM

TROPOPAUSE

TEMPERATURE

MOISTURE

FREE ATMOSPHERE

1 KM — $Z_1$

MARINE INVERSION
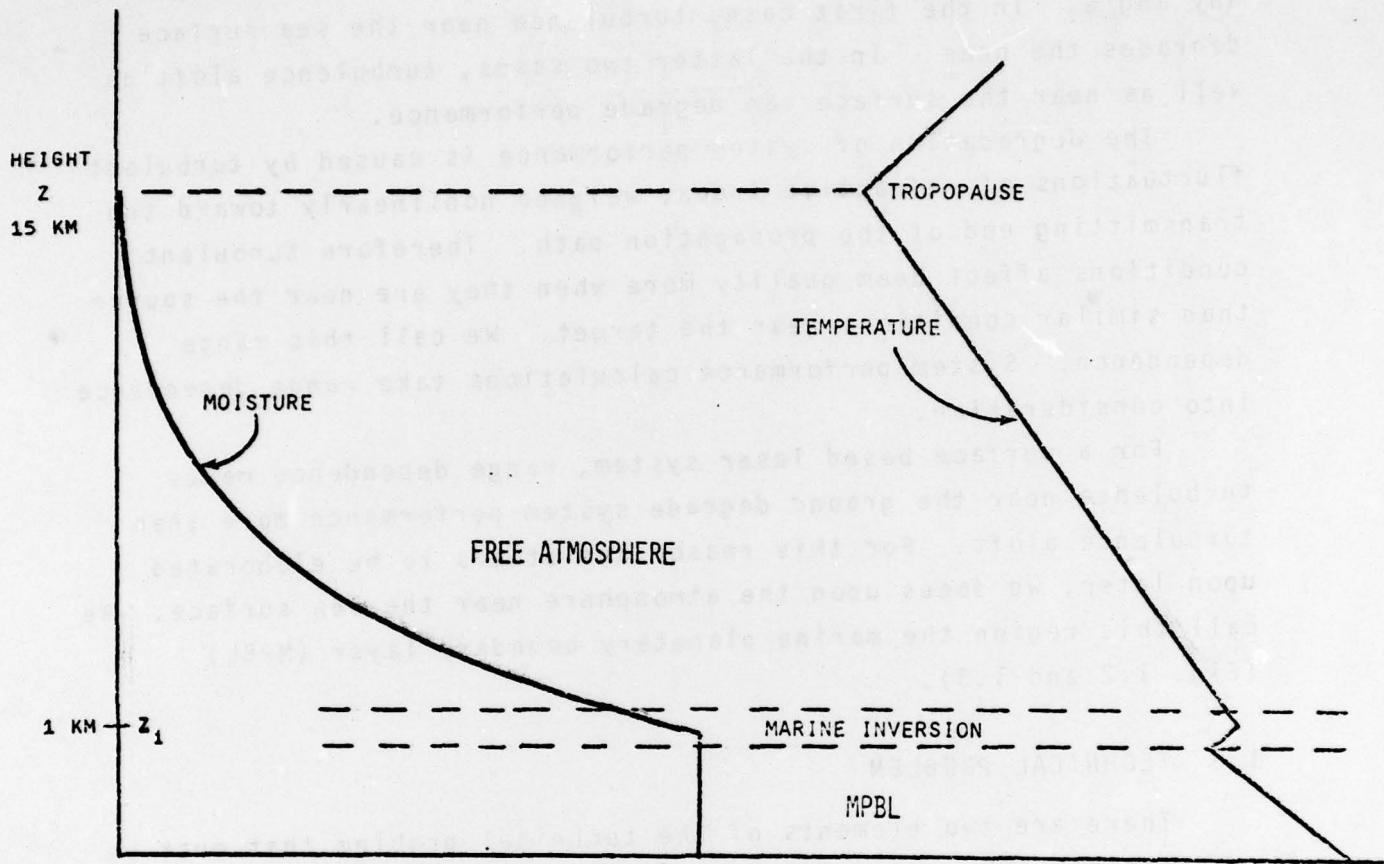
MPBL

Fig. 1.2 Schematic Marine Atmosphere Temperature and Moisture Structure. The vertical scale is non-linear to allow more detail in the marine planetary boundary layer (MPBL). The MPBL is typically approximately 1 km thick, well mixed as evidenced by constant mixing ratio and capped by a stable marine inversion at a height $Z_1$. The free atmosphere extends from the marine inversion to the tropopause and is characterized by minimal turbulent mixing.

4

FREE ATMOSPHERE

$Z_i$ _____

UPPER MPBL

$.1 Z_i$ — — — — — — — — — — — — —
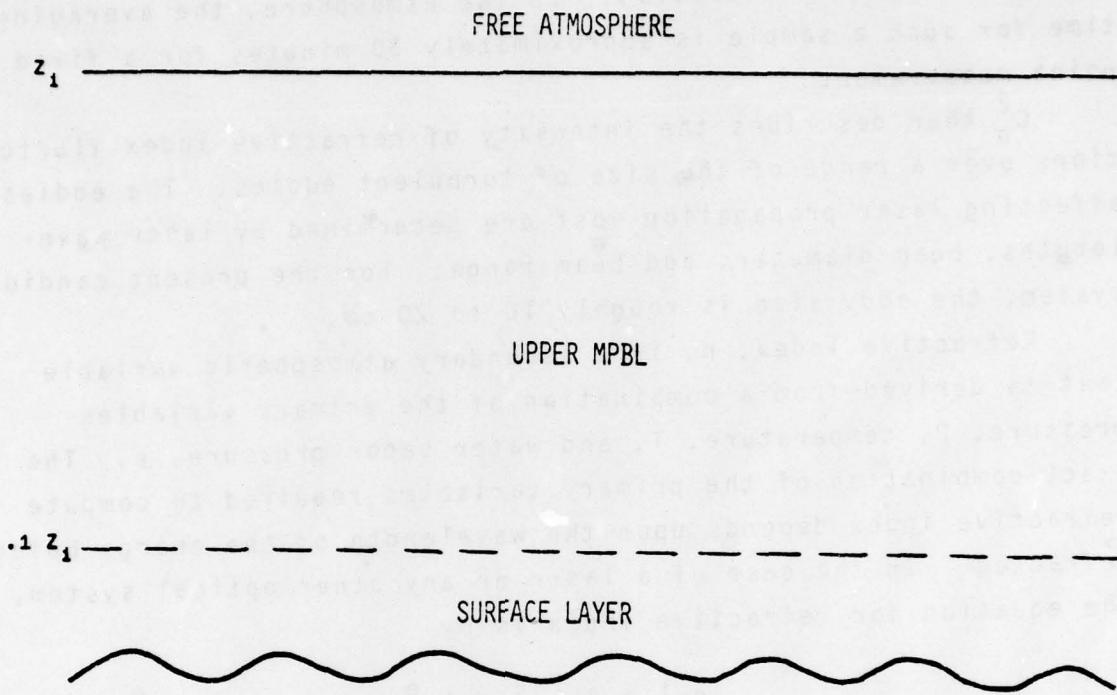
SURFACE LAYER

Fig. 1.3  Marine Planetary Boundary Layer (MPBL).  The surface
layer is approximately 10% of the MPBL and is a region of
surface forced mixing.  The upper MPBL is influenced by both
surface forcing and free atmospheric effects.  $Z_i$ is the
height of the marine inversion that caps the MPBL.

5

n(x+r) and n(x) in (1.1) are refractive index at points in space separated by a short distance, r, and the overbar represents an average over enough time and/or space to obtain a statistically stable sample of fluctuation. In the atmosphere, the averaging time for such a sample is approximately 30 minutes for a fixed point measurement.

$C_n^2$ then describes the intensity of refractive index fluctuations over a range of the size of turbulent eddies. The eddies affecting laser propagation most are determined by laser wavelengths, beam diameter, and beam range. For the present candidate system, the eddy size is roughly 10 to 20 cm.

Refractive index, n, is a secondary atmospheric variable that is derived from a combination of the primary variables pressure, P, temperature, T, and water vapor pressure, e. The exact combination of the primary variables required to compute refractive index depends upon the wavelength of the energy being refracted. In the case of a laser or any other optical system, the equation for refractive index is by

$$n - 1 = A_1 \frac{P-e}{T} + A_2 \frac{e}{T} \qquad (1.2)$$

where

$$A_1 = 78.7 \times 10^{-6} K \ mb^{-1} \text{ and } A_2 = 66.3 \times 10^{-6} K \ mb^{-1}.$$

Since refractive index is related to temperature and moisture, the fluctuations in refractive index that compose $C_n^2$ are similarly composed of fluctuations in temperature moisture and pressure. The effect of pressure fluctuations can be neglected. The fluctuations of temperature and moisture are described by temperature structure parameter, $C_T^2$, moisture structure parameter, $C_e^2$, and a structure parameter relating the two called temperature/moisture structure parameter, $C_{eT}$.

The relationship between the individual component structure parameter and $C_n^2$ is

$$C_n^2 = B_1 C_T^2 + B_2 C_{Te} + B_3 C_{eT}^2 \qquad (1.3)$$

6

where $B_1$, $B_2$, and $B_3$ are functions of temperature pressure, vapor pressure.

Over the range of normally observed values of the various structure parameters, $C_T^2$ is the largest contributor to $C_n^2$. Over land, where moisture sources are more remote and relatively small, the contributions by $C_e^2$ and $C_{eT}$ are negligible.

Most observational studies of the structure parameter have been made over land. Consequently, of the three structure parameters, we know the most about $C_T^2$. Because the contribution of the other structure parameters is negligible over land anyway, $C_n^2$ is solely determined by $C_T^2$ over land (e.g., over White Sands Missile Range).

Over water, however, the contributions of the moisture structure parameters are significant. When we desire $C_n^2$, we can observe and/or calculate $C_T^2$ and then adjust it for the contribution made by fluctuations in moisture.

### 1.3.2 Atmospheric Layers

The marine atmosphere is composed of two layers; the marine planetary boundary layer, previously defined as the MPBL, and the free atmosphere. The MPBL extends from the ocean surface to a stable region typically about 1 km above the surface that we call the marine inversion. The free atmosphere extends from the marine inversion to the tropopause, another stable region at a height of approximately 15 km. Figure 1.2 shows a schematic marine atmospheric temperature and moisture sounding showing the MPBL, marine inversion, free troposphere and tropopause.

### 1.3.2.1 Free troposphere

Motion in the free atmosphere is controlled by large scale temperature gradients. On the global scale, air rises near the equator, cools as it moves north and descends in the mid latitudes. On a synoptic scale in the Northern Hemisphere, air moves clockwise around and descends in high pressure systems, and moves counterclockwise around and ascends in low pressure centers.

7

Surface effects exert little or not influence on motion in the free troposphere. With the exception of clear air turbulence (CAT), there is little atmospheric turbulence in the free troposphere. Turbulent fluctuations of refractive index, are weak in the free troposphere and consequently $C_n^2$ values are low in this region, except possibly near CAT. Since CAT accompanies strong wind shears and sharp temperature discontinuities, CAT occurs less than 20% of the time.

Potential Navy HEL weapons are intended to operate from ships. Since turbulence effects on HEL systems performance are range dependent, MPBL turbulence is the primary turbulence influence on laser propagation, while effects of the free atmosphere are minimal. For this reason, the NEPRF workshop considered only MPBL turbulence. The workshop did not consider free atmosphere turbulence nor will we review it in this report.

We suggest, however, that a search be made of the literature to confirm the conditions for low values of $C_n^2$ in the free troposphere and that HEL system performance calculations of the effects of different levels of $C_n^2$ at free troposphere distances from the weapon be made to confirm the basic premises upon which we excluded the free troposphere from this report.

1.3.2.2 Marine planetary boundary layer

In contrast to the free troposphere, motion in the MPBL is only weakly influenced by large scale temperature discontinuities and is heavily influenced by surface effects. The primary surface effects are heating or cooling and friction.

Surface effects cause the PBL to be highly turbulent. Surface heating causes buoyancy generated turbulence and wind shear causes mechanically generated turbulence.

The MPBL can be divided into a layer in immediate contact with the surface, called the surface layer, and the layer above that up to the marine inversion, called the upper MPBL. The surface layer comprises approximately 10% of the MPBL and experiences almost no free tropospheric influence. The upper MPBL can be thought of as a transition layer between the surface layer and

8

the free atmosphere, where both surface forcing and synoptic scale features influence $C_n^2$. Figure 1.3 is a schematic representation of the marine PBL showing the relative depth of the surface layer and the upper MPBL.

1.3.2.2.1  Surface layer. Scaling laws relating $C_n^2$ to bulk meteorological parameters in the surface layer have been successfully studied for a number of years and are well defined.

Section 2 of this report describes surface layer scaling laws and describes a sequence of calculations to compute $C_n^2$ from shipboard measurements of air temperature, relative humidity, wind speed and sea surface or bucket temperature.  It was the consensus of the workshop that the surface layer scaling laws predict to a factor of two.  Further refinement is unjustified because the accuracy of the shipboard observations introduces the same order of uncertainty into $C_n^2$.

1.3.2.2.2  Upper MPBL. Scaling laws in the upper MPBL are only qualitatively known.  Many of the relevant physical processes that control turbulent fluctuations in the upper MPBL are understood; however, several are not.  The largest unknown influences are those that feed down from the free atmosphere.

In the upper MPBL, two avenues of approach are available to link $C_n^2$ to bulk meteorological variables:  (1) scaling laws can be developed to the point where they are as well accepted as those in the surface layer; or (2) scaling laws can be abandoned in favor of dynamic models of the upper MPBL that calculate $C_n^2$ directly from first principles.

Chapter 3 of this report describes the current status of both scaling laws and dynamic models in the upper MPBL.  It concludes that considerable progress needs to be made to improve scaling laws, and to verify, and probably improve, dynamic models in the upper MPBL.  It further concludes that dynamic models may be used to develop improved scaling laws in lieu of large numbers of observations.

## 2.  ESTIMATION OF REFRACTIVE INDEX STRUCTURE PARAMETER IN THE SURFACE LAYER FROM BULK METEOROLOGICAL MEASUREMENTS

### 2.1  INTRODUCTION

Modern turbulence theory provides a good description of fluctuations of wind, temperature and humidity in the atmospheric surface layer, i.e., the layer of the atmosphere within 50 m to 100 m of the surface. With this theory, the relevant turbulence parameter, $C_n^2$, is related to commonly observed meteorological measurements, such as temperature and wind, by well accepted scaling laws. A preliminary NEPRF model that incorporated these scaling laws in a continental environment was supplied to the workshop and is included as Appendix C. The following paragraphs present a summary of the scaling laws and how they are adapted to the marine environment.

Paragraphs 2.2 through 2.8 describe the relationships of $C_n^2$ to a progression of physical scaling laws which eventually depend on observable meteorological measurements. Paragraph 2.9 describes the modification of one measured parameter, sea surface temperature from the bucket measurement, to actual sea surface temperatures. Paragraph 2.10 summarizes the values of empirical constants in the calculation. A method of calculation, with a flow diagram, are included in Para. 2.11. The problem of intermittency of $C_n^2$ is addressed in Para. 2.11. Recommendations for the modification of the NEPRF preliminary model are presented in Para. 2.12.

### 2.2  REFRACTIVE INDEX STRUCTURE PARAMETER, $C_n^2$

Earlier we have stated that $C_n^2$ depends principally on the temperature structure parameter, $C_T^2$, with a modification for humidity fluctuations and the correlation of humidity and temperature fluctuations. At the NEPRF workshop, two alternative formulations of the humidity modification were presented. The first, introduced by Wesely, modifies $C_T^2$ by a function involving moisture and the correlation of moisture and temperature

11

fluctuations. The second approach, introduced by Panofsky, uses conventional surface layer scaling laws to derive the moisture modification of $C_n^2$.

Both methods lead to a modification of temperature structure function to account for humidity. When temperature and moisture fluctuations are perfectly correlated, the modifications are identical. If the correlation is not perfect, Wesely indicates a smaller humidity correction than Panofsky.

The importance of the existence of two derivations is in their independent verification of the maximum change of $C_T^2$ to account for moisture. Together with experimental verification by Friehe (1977) and Davidson et al. (1978), these derivations justify confidence in the calculation of the moisture modification to $C_n^2$.

Wesely (1976) has proposed an approach to evaluating the influence of humidity on $C_n^2$. Using the relationship of the refractive index of air to pressure, temperature, and vapor pressure introduced in 1.5.1, he expands the definition of refractive index structure parameter in terms of temperature and specific humidity structure functions, $C_T^2$ and $C_e^2$, and the correlation of temperature and vapor pressure, $C_{eT}$.

These two expressions are combined to provide $C_n^2$ as a function of the requisite structure functions and covariances,

$$
C_n^2 = C_T^2 \left(\frac{A_1 P}{T}\right)^2 \alpha_v^2 ; \quad \alpha_v^2 = 1 + 2r_{eT}\left[\frac{(1-A_2/A_1)C_e T}{PC_T}\right] + \left[\frac{(1-A_2/A_1)C_e T}{PC_T}\right]^2 \quad (2.1)
$$

where T is mean layer temperature, P is mean layer pressure $A_1 = 78.7 \cdot 10^{-6} K\ mb^{-1}$, $A_2 = 66.7 \cdot 10^{-6} K\ mb^{-1}$ and $r_{eT} = \frac{C_{eT}}{C_e C_T}$.

This relation becomes simple when $r_{eT} = 1$, that is e, T are perfectly correlated,

$$
C_n^2 = C_T^2 \left(\frac{A_1 P}{T}\right)^2 \left(1 + \frac{0.03}{B}\right)^2 \quad (2.2)
$$

Until $r_{eT}$ is better related to atmospheric parameters, we recommend using $r_{eT}$ equal to 1 and hence Eq. (2.2).

12

Panofsky proposed an alternative derivation. Based on surface layer scaling laws, the derivation does not explicitly use the temperature-humidity correlation, $C_{eT}$, but ends with the same expression as Eq. (2.2). The derivation is shown in Appendix D.

## 2.3 TEMPERATURE STRUCTURE PARAMETER $C_T^2$

The temperature structure parameter $C_T^2$ is defined in a similar way to the definition of $C_n^2$ provided in 1.5.1,

$$C_T^2 = \overline{[T(x+r) - T(x)]^2} \, r^{-2/3} \qquad (2.3)$$

where $T(x)$ is the temperature at point x, and the remaining notation is the same as in 1.5.1. In the surface layer, dimensional arguments first introduced by Monin and Obukhov can be used to relate $C_T^2$ to a temperature scale, $T_*$, a height z, and a stability function $g(z/L)$,

$$C_T^2 = T_*^2 \, z^{-2/3} \, g(z/L) \qquad (2.4)$$

where L is the Monin-Obukhov length scale.

## 2.4 STABILITY FUNCTION IN $C_T^2$

Using a set of careful observations over uniform terrain in Kansas, Wyngaard et al. (1971) have empirically determined the function $g(z/L)$ from measurements of $C_T^2$ and the scaling parameters L and $T_*$. The results have been tested over water by Friehe (1977) and Davidson et al (1978). As a result, the following expressions are recommended:

$$g(z/L) = 4.9(1-7z/L)^{-2/3} \qquad (L \leq 0)$$

$$\qquad\qquad\qquad\qquad\qquad\qquad (2.5)$$

$$g(z/L) = 4.9(1+2.75(z/L)^b) \qquad (L \geq 0)$$

where the exponent b has been suggested either as 1 or .667.

13

## 2.5 SCALING FUNCTIONS IN THE SURFACE LAYER

The Monin-Obukhov theory describes the surface layer using non-dimensional atmospheric variables. Physical variables of length, z, wind speed U, temperature T, and specific humidity q are made non-dimensional by defining scaling length, L, scaling speed $U_*$, a scaling temperature $T_*$ and a scaling humidity $Q_*$. The non-dimensional parameters describe the fluxes of momentum, heat, and humidity in the surface layer.

### 2.5.1 <u>Monin-Obukhov Length, L</u>

In a dry atmosphere the characteristic length $L_{DRY}$ is taken as the Monin-Obukhov length,

$$L_{DRY} = \frac{T U_*^2}{g k T_*} \qquad (2.6)$$

where T is mean surface layer temperature, g is acceleration of gravity, and k is the von Karman constant. In unstable air buoyancy generated turbulence dominates at levels above -L, while mechanical turbulence dominates much below -L. The length is corrected for moisture by using the Bowen ratio B,

$$L = L_{DRY} \left(1 + \frac{.07}{B}\right)^{-1} \qquad (2.7)$$

The Bowen ratio is related to the heat and moisture fluxes and is expressed in terms of the scaling temperature and humidity,

$$B = \frac{C_p T_*}{L_w Q_*} \qquad (2.8)$$

where $C_p$ is specific heat of air at constant pressure and $L_w$ is latent heat of vaporization.

### 2.5.2 Scaling Wind Speed $U_*$, Temperature $T_*$, and Humidity $Q_*$

The surface layer is characterized by fluxes of momentum, heat and moisture which are independent of height. These constant fluxes are used to define scaling velocity $U_*$, temperature $T_*$, and humidity $Q_*$,

14

$$T_* = - \frac{1}{U_*} \overline{T'w'}$$

$$U_* = \sqrt{-\overline{U'w'}} \qquad\qquad\qquad (2.9)$$

$$Q_* = - \frac{1}{U_*} \overline{q'w'}$$

where U', T' and q' are fluctuations of horizontal wind, tempera-
ture and humidity about their means, and the overbar is an average
among all fluctuations. These scaling variables are related to
the vertical profiles of each variable,

$$U_* = kU[\ln(\frac{Z}{Z_0}) - \psi_M(z/L)]^{-1}$$

$$Q_* = \frac{k}{R}(q-q_s)[\ln(\frac{Z}{Z_{0Q}}) - \psi_Q(z/L)]^{-1} \qquad (2.10)$$

$$T_* = \frac{k}{R}(T-T_s)[\ln(\frac{Z}{Z_{0T}}) - \psi_H(z/L)]^{-1}$$

This is the first time that bulk parameters are introduced.
The necessary bulk parameters are wind speed U, normally taken at
10 m height; air temperature T, again at 10 m, air temperature at
the surface $T_s$, taken to be the sea surface temperature; q,
specific humidity at 10 m; and $q_s$, specific humidity at the sea
surface. Together with these bulk parameters, newly derived
parameters have been introduced. The $Z_0$, $Z_{0T}$, and $Z_{0Q}$ are rough-
ness parameters describing molecular transport of wind, temperature,
and moisture near the surface, and $\psi_M$, $\psi_H$, and $\psi_Q$ are empirical
profile functions. A new constant R is included in the equations
for temperature and humidity. The value of this constant is
accepted as 0.74 based on reliable field experiments.

## 2.6   PROFILE FUNCTIONS

We adopt the profile functions, $\psi$, as formulated by Businger
et al. (1971). These functions have been verified both over land
and over water. These functions are

15

$$\psi_M = \ln\left[\left(\frac{1+x^2}{2}\right)\left(\frac{1+x}{2}\right)^2\right] - 2 \text{ arc } \tan(x) + \pi/2 \qquad \psi_M = -\beta\frac{z}{L}$$

$$x = (1 - \gamma_m \, z/L)^{1/} \tag{2.11}$$

$$\psi_H = \psi_Q = 2 \ln\left[\frac{1 + \sqrt{1 - \gamma_H \frac{z}{L}}}{2}\right] \qquad \psi_H = \psi_Q = -\frac{\beta}{R}\frac{z}{L}$$

Constants in these formulations are determined by fitting the formulations to data, and correspond best to one particular data set. Universal constants have so far not been found.

The hypothesis that the $\psi$ are the same for heat and moisture is based mostly on measurements over land. There is considerable controversy whether the assumption is valid over the ocean; but no better hypotheses are available. Fortunately, in all equations, the $\psi$'s are small compared to the logarithmic terms, so that extreme accuracy in the $\psi$'s is not required. Further, $\psi_Q$ occurs only in the correction of L for moisture, which itself is usually a small correction.

## 2.7 ROUGHNESS LENGTHS $Z_o$, $Z_{oT}$, $Z_{oQ}$

The molecular transport of momentum, heat and moisture near the surface is described by the values of $Z_o$, $Z_{oT}$, and $Z_{oQ}$ respectively. In the marine environment, the roughness lengths have values on the order of 1 mm or less. The dependence of $C_n^2$ on $Z_o$ is included primarily in the function $\ln\frac{Z}{Z_o}$, where Z is elevation, roughly 10 or 20 meters. Therefore, $C_n^2$ is not very sensitive to errors in $Z_o$, although this point should be verified.

The simplest assumption is that all these roughness lengths are equal. It was judged by the workshop participants that this assumption is too limiting, and separate treatments of $Z_o$, $Z_{oT}$ and $Z_{oQ}$ are necessary. One possible approach is the technique developed by Liu (1978). Liu has derived relations between U and $U_*$ and the transfer coefficients for momentum, heat, and moisture. Transfer coefficients for momentum, heat ($C_D$, $C_H$, $C_Q$), and moisture are directly related to the roughness lengths,

16

$$\ln(z/Z_O) = \frac{k}{C_D^{\frac{1}{2}}} + \psi_M(z/L)$$

$$\ln(z/Z_{OT}) = \frac{k}{R} \frac{C_D^{\frac{1}{2}}}{C_H} + \psi_H(z/L) \tag{2.12}$$

$$\ln(z/Z_{OQ}) = \frac{k}{R} \frac{C_D^{\frac{1}{2}}}{C_Q} + \psi_Q(z/L)$$

where z is 10 m. The derived relationships are displayed in Fig. 2.1. The values of the roughness lengths cannot be obtained in closed form expressions, and the following technique is recommended:

a. $Z_O$, $Z_{OT}$, $Z_{OQ}$ at neutral are found directly from the curves of Fig. 2.1, using the value of 10 m wind.

b. After stability corrections and $U_*$ are calculated, a new set of roughness lengths is found from Figure 2.1 using the roughness Reynolds number,

$$R_r = \frac{Z_O U_*}{\nu} \tag{2.13}$$

where $\nu$ is the kinematic viscosity of air.

## 2.8 SEA SURFACE TEMPERATURE, $T_S$

The $C_T^2$ can now be evaluated in terms of bulk meteorological parameters, and one other parameter surface temperature, $T_S$, not normally observed.

In most cases, bucket temperature, $T_W$, rather than the surface temperature is measured. We estimate $T_S - T_W$ from the theory by Liu (1978). Liu, (Fig. 2.2), gives $T_S - T_W$ as a function of the wind speed and the difference between bucket temperature and air temperature at 10 m height, $\Delta T$. In practice, temperatures at any height between 7 m and 20 m should be satisfactory in place of the temperature at 10 m.

Liu's diagram is approximated by a set of equations which should be more usable for computation than his figure. These equations are:
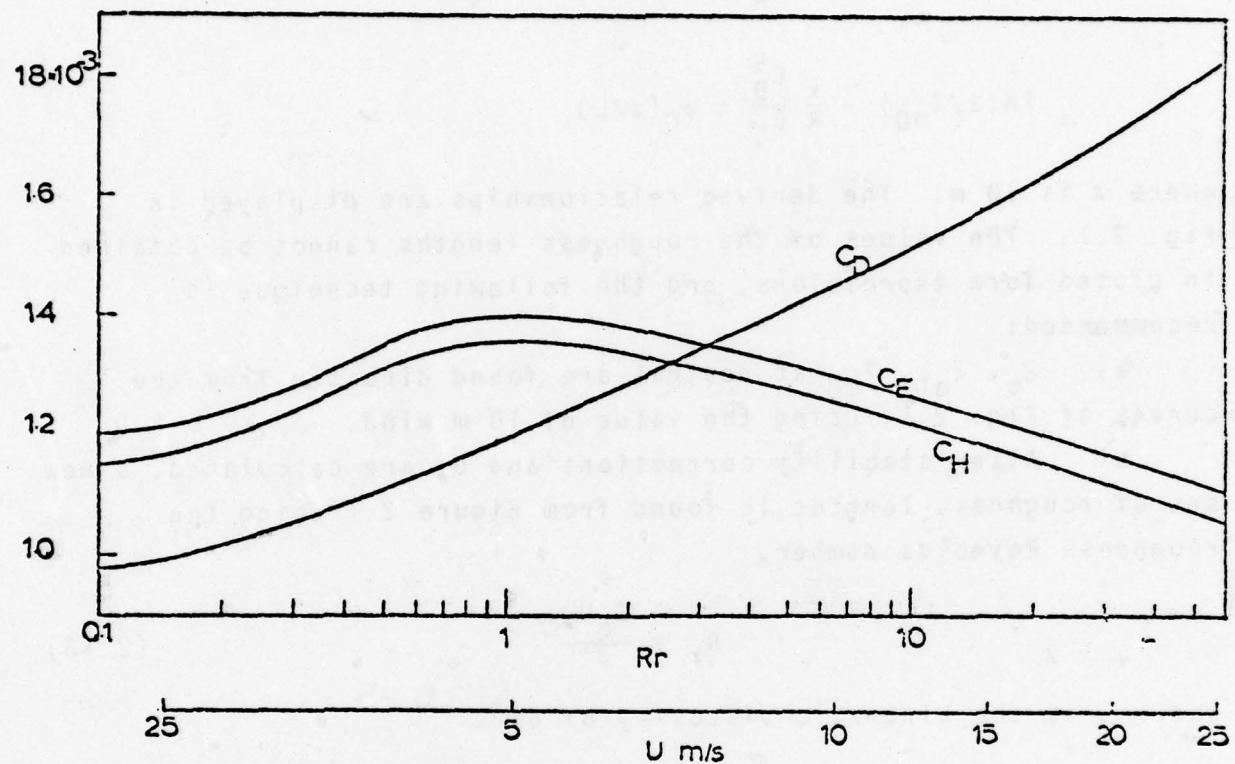
Fig. 2.1. Bulk Transfer Coefficients at Neutral Conditions Versus
10 m Wind U and Roughness Reynolds Number $R_r$ (Liu, 1978).
The transfer coefficients are approximately calculated from
wind U; when scaling speed U* and roughness length $Z_o$ are
found, transfer coefficients are found from $R_r$ using formulas
in text.

18
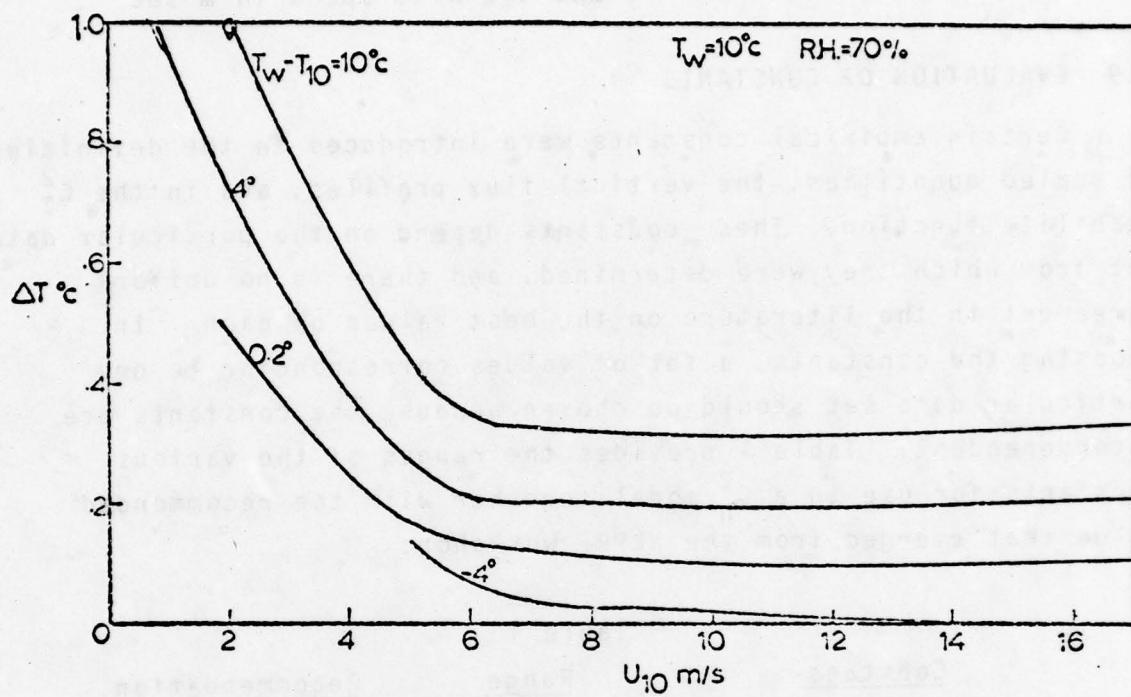
Fig. 2.2 Temperature Difference Across the Aqueous Sublayer Versus 10 m Wind for Values of Air-Bulk Water Temperature Difference $T_w - \bar{T}_{10}$ (Liu, 1978). These formulas account for radiation and molecular effects in the surface layer.

$$T_w - T_s = .025\Delta T + 0.1 \qquad (U > 6 \text{ m sec}^{-1})$$ (2.14)

$$T_w - T_s = 0.1\Delta T + .8 - U(.117 + .0125\Delta T) \ (U < 6 \text{ m sec}^{-1})$$

where the temperature is in °C and the wind speed in m sec$^{-1}$.

## 2.9  EVALUATION OF CONSTANTS

Certain empirical constants were introduced in the definition of scaled quantities, the vertical flux profiles, and in the $C_T^2$ stability function.  These constants depend on the particular data set from which they were determined, and there is no uniform agreement in the literature on the best values of each.  In choosing the constants, a set of values corresponding to one particular data set should be chosen because the constants are interdependent.  Table 1 provides the ranges of the various constants for use in a $C_n^2$ model together with the recommended value that emerged from the NEPRF workshop.

Table 1

| Constant | Range | Recommendation |
|---|---|---|
| For Scaling Functions | | |
| k | 0.33-0.41 | 0.37 |
| R | .74-1 | .74 |
| For Profile Functions | | |
| $\gamma_m$ | 15-16 | 15 |
| $\gamma_H$ | 9-18 | 9 |
| $\beta$ | 4.7 | 4.7 |
| For Stability Function | | |
| b | .667-1 | 1. |

## 2.10  CALCULATION OF $C_n^2$

The calculation of $C_n^2$ proceeds using the equations described in Paras. 2.2 through 2.8 and the constants given in Para. 2.9. The step-by-step procedure is as follows:

a.  Modify the sea surface temperature measurement to an actual sea surface temperature value using Eq. (2.14) and $T$, $T-T_w$ and $U$.

b.  Set initial stability to neutral, i.e., $z/L = 0$ and $\psi_M = \psi_H = \psi_Q = 0$.

c.  The bulk wind speed determines an initial value of $C_D$, $C_H$, $C_Q$ from Fig. 2.1.

d.  Calculate $Z_o$, $Z_{oT}$, and $Z_{oQ}$ from $C_D$, $C_H$, $C_Q$ with Eq. (2.12).

e.  Evaluate scaling parameters $U_*$, $T_*$ and $Q_*$ using Eq. (2.10).

f.  Evaluate Bowen ratio, $B$, using Eq. (2.8).

g.  Evaluate Monin-Obukhov length for moist atmosphere using Eqs. (2.6) and (2.7).

h.  Test if the new $L$ is within 1% of old value of $L$.  If so, go to statement l.  If not, go to statement i.

i.  Calculate stability functions $\psi_M$, $\psi_H$, $\psi_Q$ using Eq. (2.11).

j.  Calculate rougnness Reynolds number $Rr$ from Eq. (2.13).

k.  Evaluate $C_D$, $C_H$, $C_Q$ from Fig. 2.1 using $Rr$ and go to statement d.

l.  Evaluate $C_T^2$ stability function ($g(z/L)$ using Eq. (2.5).

m.  Evaluate $C_T^2$ using Eq. (2.4).

n.  Calculate $C_n^2$ using Eq. (2.2).

This procedure is graphically outlined in Fig. 2.3.

## 2.11 DEVIATION OF $C_n^2$ FROM ENSEMBLE MEAN VALUE

The values of $C_n^2$ predicted by the surface model are values of mean turbulent quantities.  The equations were derived from measurements of temperature fluctuations of one turbulent eddy size at one point averaged over long periods of time, i.e., 20 to 30 minutes.  The laser system, on the other hand, is affected by turbulence over a spectrum of eddy sizes and operates over a short time period, about 10 seconds, and over a long path, about 10 km.

Bulk $u, T, T_w, e$

SFC Temp. Fig. 2.2

All $\psi = 0$ $L = \infty$

$C_D, C_H, C_Q$ Fig. 2.1

$Z_0, Z_{0T}, Z_{0Q}$ Eq. 2.12

$U_*, T_*, Q_*$ Eq. 2.10

$B$ Eq. 2.8

$L_{NEW}$ Eq. 2.6, 2.7

$\left|\dfrac{L_{NEW} - L}{L_{NEW}}\right| < 01$

N

$Z_0, Z_{0T}, Z_{0Q}$ Eq. 2.12

$C_D, C_H, C_Q$ Fig. 2.1

$R_r$ Eq. 2.13

$\psi_M, \psi_H, \psi_Q$ Eq. 2.11

$g(z/L)$ Eq. 2.5

$C_T^2$ Eq. 2.4

$C_n^2$ Eq. 2.2

$C_n^2$
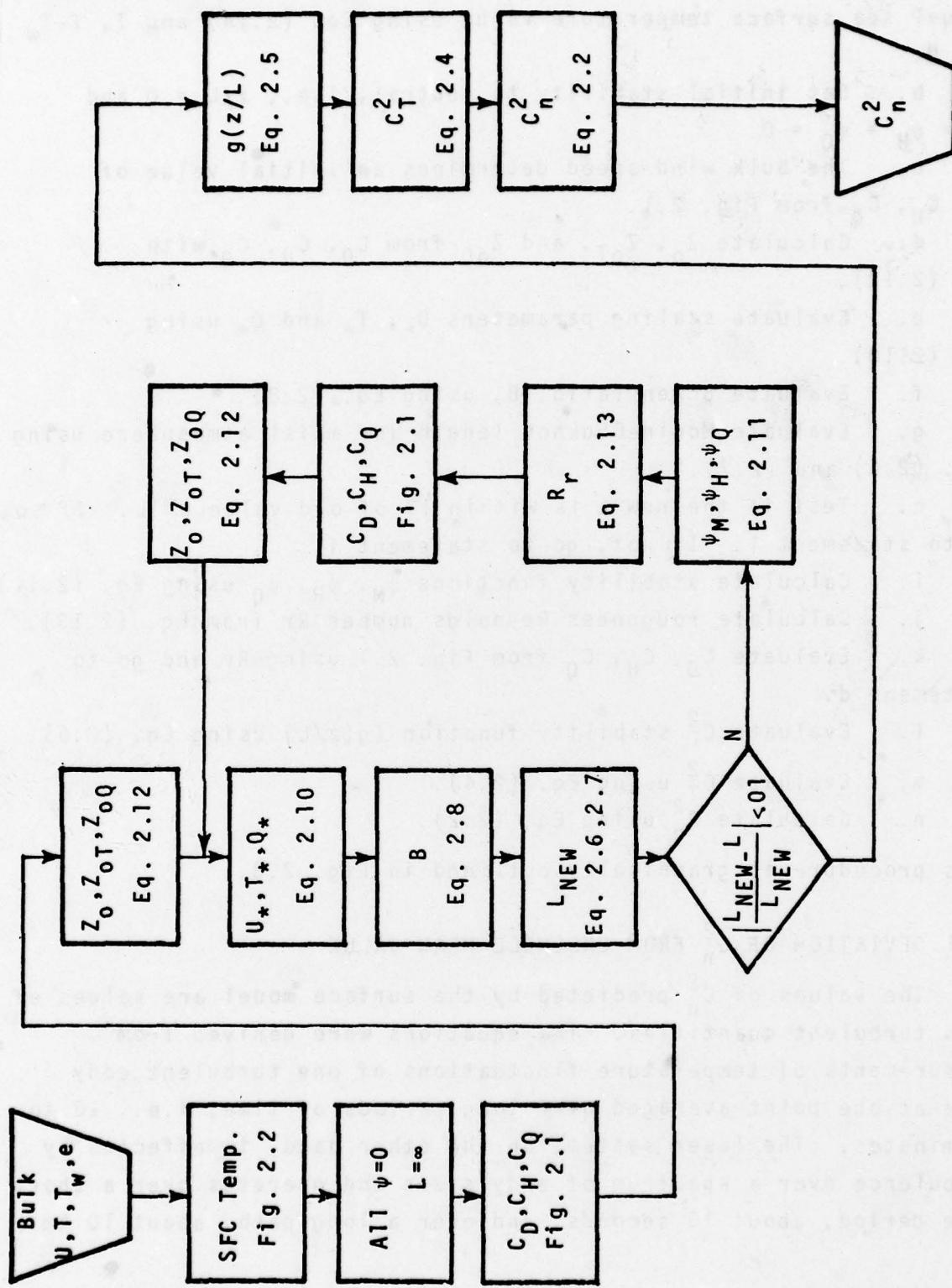
Fig. 2.3. Flow Chart of Surface Layer $C_n^2$ Calculation. Symbols, equation numbers, and figure numbers are those used in text.

The averaging time to obtain mean fluctuations of refractive index is proportional to the relevant eddy size, and inversely proportional to the wind speed. In the case of the measurements on which the scaling laws are based, the eddy size corresponds to a temperature probe separation r, about 20 cm. Therefore the averaging time, $T_s$, relevant to the scaling laws is

$$T_s = r/U . \qquad (2.15)$$

In the case of an optical system, the eddy size corresponds to a combination of wavelength $\lambda$ and range R. Therefore averaging time $T_{op}$ for the optical system is

$$T_{op} = \sqrt{\lambda R/U} . \qquad (2.16)$$

Wyngaard and Clifford (1978) show that the mean $C_n^2$ corresponding to the two methods are the same if

$$T_s/T_{op} = \frac{144}{\sqrt{\lambda R}} . \qquad (2.17)$$

From this we infer that a laser beam is affected by a mean $C_n^2$ corresponding to a model prediction if the minimum time interval of the laser transmission $T_{Tr}$ satisfies

$$T_{Tr} = T_{sT} \sqrt{\lambda R/144} . \qquad (2.18)$$

For a laser of wavelength 3.5 $\mu$m, and range 10 km, and a model ensemble averaging time of 20 minutes, the equation states that the turbulence model prediction of $C_n^2$ describes the turbulence affecting the system if the laser transmission duration is at least 1.5 sec.

## 2.12 RECOMMENDATIONS - SURFACE LAYER $C_n^2$ ASSESSMENT

The surface layer $C_n^2$ model outlined here is recommended for verification and use by the HEL program to predict $C_n^2$ for within the atmospheric surface layer (within 100 m of the sea surface). The model is basically the NEPRF preliminary model (Appendix C) with the following modifications:

23

a.    Model should account for humidity using Eq. (2.2).

b.    Roughness lengths for momentum, heat, and moisture should be treated as different functions, as discussed in Para. 2.7.

c.    Sea surface temperature should be derived from bucket sea surface temperature measurement using Eq. (2.14).

The humidity modification has not been verified in the marine atmosphere.  A limited field program should be conducted to verify the recommended modification of $C_T^2$ to produce $C_n^2$.

## 3. REFRACTIVE INDEX STRUCTURE PARAMETERS: PROFILES IN THE UPPER MARINE PLANETARY BOUNDARY LAYER

### 3.1 INTRODUCTION

We now discuss methods of computing vertical profiles of refractive index structure parameters above the surface layer. In particular, this chapter is concerned with that portion of the atmosphere between the top of the surface layer and the top of the marine planetary boundary layer (MPBL). We term this atmospheric region the upper MPBL.

Chapter 2 presents well-established Monin-Obukhov scaling laws that yield $C_n^2$ within the surface boundary layer. The scaling laws change, however, as one moves to higher altitudes. The mechanical surface turbulence becomes less important than surface heating and the influence of the inversion. The stability of the MPBL, furthermore, may profoundly alter the nature of the scaling laws in the upper MPBL.

When the MPBL is stable (L>0), no adequate theory exists for scaling atmospheric variables in the upper MPBL. This is an area of active research; new theories can be expected to emerge. When the MPBL is unstable (L<0), there are scaling laws for the upper MPBL. These scaling laws, however, require knowledge of universal functions analogous to the universal function g(z/L) that occurs in the expression for $C_T^2$ in the surface layer. These universal functions in the upper MPBL are unknown currently. The scaling laws for the upper MPBL remain qualitative.

Upper MPBL scaling is detailed in Para. 3.2. In Para. 3.3 we discuss numerical MPBL models and how they can contribute to the study of structure parameter profiles. Observational data, primarily from instrumented aircraft, are discussed in the following section. In the final section, we recommend methods of obtaining a better understanding of $C_n^2$ in the upper MPBL.

## 3.2 SCALING LAWS IN THE UPPER MPBL UNDER UNSTABLE CONDITIONS

### 3.2.1 Regions of Validity

The depth of the MPBL is generally defined by the inversion height, $Z_i$. In the surface layer, where $Z < 0.1 Z_i$, Monin-Obukhov scaling has been adequately confirmed under a variety of circumstances. Near the inversion, mixed layer scaling is appropriate. In this region, where $Z_i > Z > -L$, the velocity scale analogous to $U_*$ in the surface layer is $W_*$ and the temperature scale analogous to $T_*$ in the surface layer is $\theta_*$, where

$$W_* = \left( \frac{g H z_i}{\rho C_p T} \right)^{1/3} ,$$

$$\theta_* = \frac{H}{\rho C_p W_*} , \qquad (3.1)$$

and H is the surface heat flux; $\rho$, atmospheric density; and $C_p$, the specific heat at constant pressure.

Between the two regions, the nature of the scaling depends on the strength of shear production relative to the strength of buoyant production of turbulence. When buoyant production is dominant in the surface layer, characterized by $-L < 0.1 Z_i$, the two scaling regions overlap. The overlap region, $-L < Z < .1 Z_i$, is termed a layer of free convection. Here, Monin-Obukhov and mixed layer scaling apply simultaneously.

In the other case, where shear production of turbulence is not negligible compared to buoyant production within the surface layer, i.e., $-L > 0.1 Z_i$, no overlap region exists. Rather, the layer $0.1 Z_i < Z < -L$ is a transition region between the Monin-Obukhov and mixed layer scaling regions where neither scaling law applies. This region is an enigma insofar as scaling is concerned. A MPBL having a free convective region and a MPBL having a transition layer are shown in the Fig. 3.1.

26
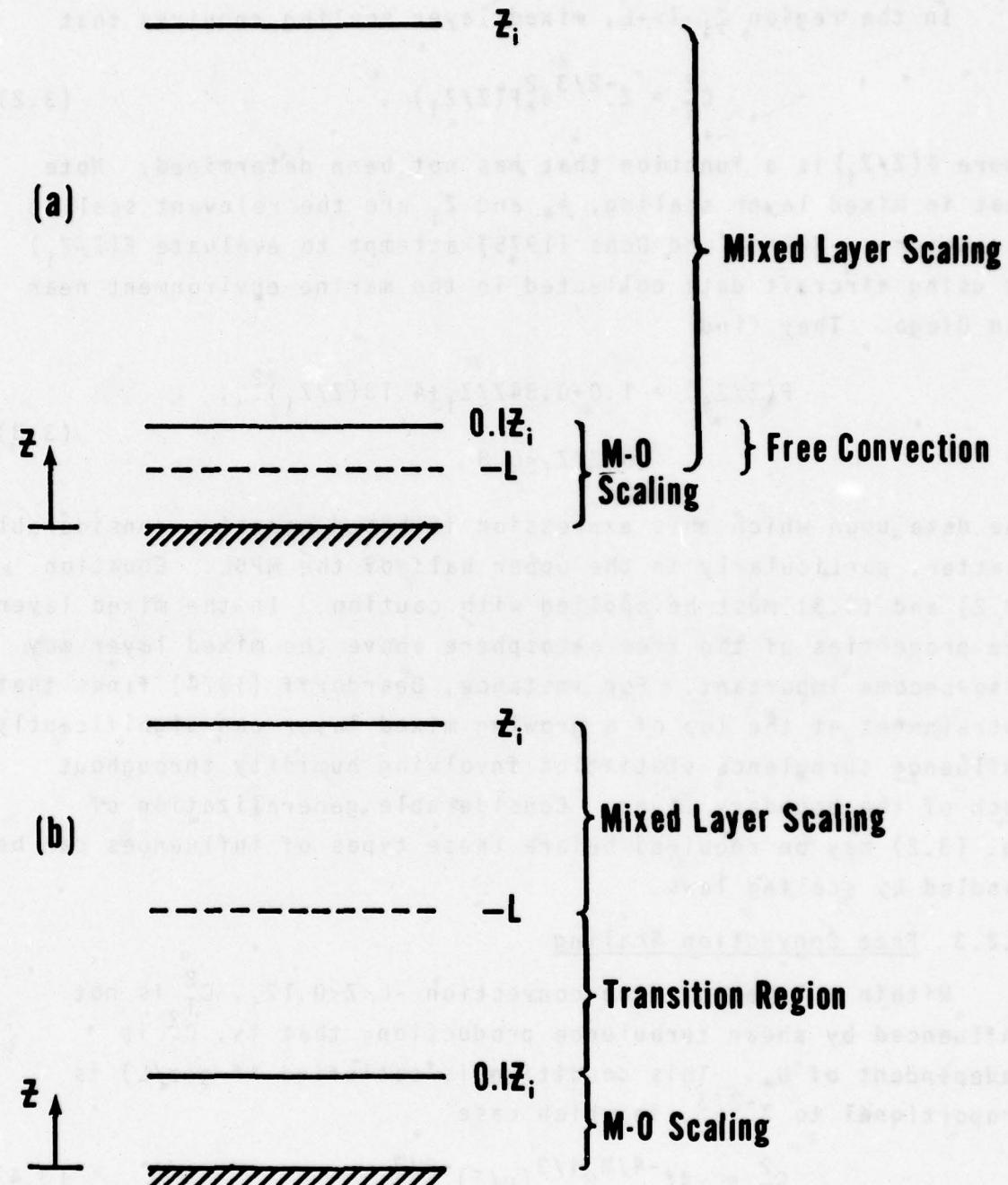
Fig. 3.1. (a) Boundary layer which has a free convection region
in which both mixed layer scaling and Monin-Obukhov (M-O)
scaling apply simultaneously; and (b) a boundary layer with
no free convection region. Neither mixed layer scaling nor
M-O scaling apply in the transition region.

### 3.2.2 Mixed Layer

In the region $Z_i > Z > -L$, mixed layer scaling requires that

$$C_T^2 = Z^{-2/3} \theta_*^2 F(Z/Z_i) , \tag{3.2}$$

where $F(Z/Z_i)$ is a function that has not been determined. Note that in mixed layer scaling, $\theta_*$ and $Z_i$ are the relevant scaling parameters. Frisch and Ochs (1975) attempt to evaluate $F(Z/Z_i)$ by using aircraft data collected in the marine environment near San Diego. They find

$$F(Z/Z_i) = 1.0 + 0.84 Z/Z_i + 4.13(Z/Z_i)^2 ,$$
$$0 < Z/Z_i \leq 0.8 . \tag{3.3}$$

The data upon which this expression is based contains considerable scatter, particularly in the upper half of the MPBL. Equation (3.2) and (3.3) must be applied with caution. In the mixed layer, the properties of the free atmosphere above the mixed layer may also become important. For instance, Deardorff (1974) finds that entrainment at the top of a growing mixed layer can significantly influence turbulence statistics involving humidity throughout much of the boundary layer. Considerable generalization of Eq. (3.2) may be required before these types of influences can be handled by scaling laws.

### 3.2.3 Free Convection Scaling

Within a layer of free convection $-L < Z < 0.1 Z_i$, $C_T^2$ is not influenced by shear turbulence production, that is, $C_T^2$ is independent of $U_*$. This condition is satisfied if $g(z/L)$ is proportional to $Z^{-2/3}$, in which case

$$C_T^2 = A Z^{-4/3} H^{4/3} (g/T)^{-2/3} , \tag{3.4}$$

where A is a constant. Within the region of applicability, this relation fits observations.

28

### 3.2.4 Transition Region

When shear production is not negligible anywhere within the surface layer, $-L > 0.1 Z_i$, scaling is complicated. The middle region of the MPBL is influenced both by surface shear turbulence production and the presence of the inversion. Here $U_*$ and $Z_i$ are important scaling parameters, and we must write

$$C_T^2 = Z^{-2/3} T_*^2 F'(Z/Z_i, Z/L) , \qquad (3.5)$$

where $F'$ is still another universal function. This scaling law transition region is quite common over the oceans. No quantitative proposal for the form of $F'$ exists.

## 3.3 NUMERICAL MPBL MODELS: CALCULATION OF STRUCTURE PARAMETERS

### 3.3.1 Basic Nature of Models

Numerical boundary layer modeling involves solving equations which describe the basic laws of fluid dynamics and atmospheric thermodynamics. These equations generally can be characterized by the expression

$$\frac{\partial \phi}{\partial t} = \text{Source/sink} + \text{mean transport} + \text{turbulent transport}$$

where $\phi$ is any one of the dependent variables. For example, if $\phi$ represents temperature, then the source/sink term would involve processes such as radiative transfer, latent heat release, etc. The mean transport term would represent temperature advection by the mean wind, and turbulence transport would involve the divergence of the turbulent heat flux.

The source/sink terms and the mean transport terms in the fundamental equations are generally treated similarly in all models. Substantial differences exist, however, in the manner in which models treat the turbulent transport terms. We will discuss these different treatments of the turbulent transport terms in more detail in this section. Here we note only that since our concern is with turbulent refractive index fluctuations, substantial attention and care must be given to the handling of the turbulent transport terms.

29

Our interest here centers upon two different types of numerical MPBL models. One type we term a subgrid-scale closure model while the other type we term a second-moment turbulent closure model.*

### 3.3.2  Subgrid-Scale Closure Models

Subgrid-scale closure models use the fundamental equations to describe all the turbulent eddies within the resolution of the grid. The smaller subgrid-scale eddies must be parameterized.

An example of a subgrid-scale closure model is that developed by Deardorff (1973). In his model, the parameterized subgrid-scale turbulent fluxes generally represent small fractions of the total fluxes. Thus, the model forecasts are not very sensitive to the manner in which the subgrid-scale is parameterized.

Because of these considerations, the subgrid-scale closure model has considerable appeal as a tool for investigating basic physical processes in the MPBL. The major disadvantage inherent in this type of model involves the computational requirements. For example, a version of the Deardorff model used to simulate an undisturbed trade wind MPBL took about 30 h computer time with a CDC 7600 to produce a 5 h model time simulation (Sommeria, 1976). This does not include any development, debugging, or preliminary testing time. The time to analyze the model results, furthermore, is comparable to that required in an extensive field experiment. Therefore, it seems prohibitive at this time to examine $C_n^2$ in a wide variety of atmospheric situations with a subgrid-scale closure model.

_____

*The term 'closure' refers to the process whereby a set of equations becomes closed, that is, the set has an equal number of equations and unknowns. We find "second-moment" closure to be more descriptive than "second-order" or "higher-order" closure because the assumptions that close the set are introduced into the equations for the second moments.

### 3.3.3 Second-Moment Closure Models

Second-moment closure models solve the fundamental equations for the total turbulent flux rather than resolving a portion of this flux by explicitly computing the turbulent flow on scales larger than the grid scale. The parameterization involved in the closure assumptions is more important here than in subgrid-scale closure models; the parameterization affects the total flux, not just that portion of the flux that is below the grid resolution. The treatment of the total turbulent flux can involve parameterization at several levels corresponding to the level of the moment closure assumptions.

These parameterizations are best seen by first considering first-moment closure, or K-theory. Here the fluxes of momentum, heat, and moisture that appear in the fundamental equations are replaced, in analogy with molecular diffusion, with terms involving the product of an eddy coefficient and a mean gradient of wind, temperature, or humidity. This is first-moment closure because the assumptions which yield a closed set are introduced into the equations for the first moments, that is, the means. First-moment closure has serious shortcomings, however, because in actuality fluxes are not so closely tied to the local gradients. The eddy coefficient, furthermore, is a function of the flow itself and, therefore, cannot <u>a priori</u> be specified.

In second-moment closure, the turbulent fluxes (the second moments of the flow) in the fundamental equations are not directly replaced as in first-moment closure. Rather, time-dependent equations describing the dynamic behavior of these fluxes are developed. These equations contain additional higher-order moment terms. These unknowns are parameterized in terms of the known variables, thereby closing the set of equations. Thus, in a second-moment closure model, one charts the progress of both the mean variables and the turbulence moments.

The upper boundary conditions of these numerical models are usually selected to be in the free atmosphere where turbulent fluxes are weak. Near the surface, Monin-Obukhov similarity theory provides boundary values. Thus, a surface layer model as discussed

31

in Chapter 2 is incorporated as a part of the lower boundary
condition in these numerical models.

### 3.3.4 Calculating $C_n^2$ with a Second-Moment Closure Model

Although sensitive to the closure assumptions, second-moment
closure models can answer some of the questions concerning the
nature of $C_n^2$ profiles throughout the MPBL. As mentioned in Chapter
2, Wesely (1976) shows that the optical structure parameter may be
written as

$$C_n^2 = \left(\frac{A_1 P}{T^2}\right)^2 \left\{ C_T^2 + \left[\frac{2(1-A_2/A_1)T}{P}\right] C_{eT} + \left[\frac{(1-A_2/A_1)T}{P}\right]^2 C_e^2 \right\} . \qquad (3.6)$$

If this equation is to be useful, we need a way of computing $C_T^2$,
$C_{eT}$, and $C_e^2$ with the closure model throughout the MPBL. We now
discuss a possible approach.

In terms of dissipation rates, the temperature and humidity
structure parameters may be written (Wyngaard et al., 1978)

$$C_T^2 = 4\beta\varepsilon_T\varepsilon^{-1/3}, \qquad C_e^2 = 4\beta\varepsilon_e\varepsilon^{-1/3}, \qquad C_{eT} = 4\gamma\varepsilon_{eT}\varepsilon^{-1/3}. \qquad (3.7)$$

Here $\varepsilon$ is the turbulent kinetic energy dissipation rate; $\varepsilon_T$ and
$\varepsilon_e$ are the dissipation rates of temperature and vapor pressure
variances, respectively; $\varepsilon_{eT}$ is the dissipation rate of temperature-
humidity covariance; and $\beta$ and $\gamma$ are constants.

The terms $\varepsilon_T$, $\varepsilon_e$, $\varepsilon_{eT}$ and $\varepsilon$ appearing in these structure
parameter relationships, also appear in the equations that form
the core of a second-moment closure model. These dissipation terms
are approximated by closure assumptions. The typical closure
assumptions for dissipation terms are

$$\varepsilon \simeq \frac{q^2}{\tau} = \frac{q^3}{\ell} , \qquad \varepsilon_e \simeq \frac{\overline{e'^2}}{\tau} = \frac{q\overline{e'^2}}{\ell} ,$$

$$\qquad (3.8)$$

$$\varepsilon_T \simeq \frac{\overline{T'^2}}{\tau} = \frac{q\overline{T'^2}}{\ell} , \qquad \varepsilon_{eT} \simeq \frac{\overline{T'e'}}{\tau} = \frac{q\overline{T'e'}}{\ell} ,$$

32

where $\tau = \ell/q$ is a turbulent time scale and $\ell$ is a turbulent length scale. Here $q^2$ is twice the turbulent kinetic energy (i.e., (i.e., $q^2 = \overline{u'^2} + \overline{v'^2} + \overline{w'^2}$). Using these expressions the structure parameters are

$$C_T^2 \, \alpha \frac{\overline{T'^2}}{\ell^{2/3}} \, , \qquad C_e^2 \, \alpha \frac{\overline{e'^2}}{\ell^{2/3}} \, , \qquad C_{eT} \, \alpha \frac{\overline{T'e'}}{\ell^{2/3}} \, . \qquad (3.9)$$

Second-moment closure models compute the evolution of $\overline{T'^2}$, $\overline{e'^2}$, $\overline{T'e'}$, and $\ell$. Thus we solve for $C_T^2$, $C_e^2$, and $C_{eT}$ using Eq. (3.9) and for optical $C_n^2$ using Eq. (3.6).

Computation of $C_n^2$ throughout the MPBL as we have been describing is the subject of a recent report by Burk (1978). He uses a one-dimensional second-moment closure model. The question of what dimensionality a model should have to adequately describe $C_n^2$ in the MPBL is the subject of the next subsection.

### 3.3.5 Multidimension vs. 1-D Models

The dimensionality of a second-moment closure model can also be an important consideration in seeking vertical structure parameter profiles. A 1-D model assumes horizontal homogenity. It cannot yield information concerning the nature of large two or three dimensional turbulent structures such as horizontal roll vortices or hexagonal cells. For this type of information, a multidimensional model is required.

Teske and Lewellen (1979) use a two-dimensional second-moment closure model to study horizontal roll vortices. They find that the upward moving region of a roll concentrates the turbulent fluctuations. This is particularly evident near the top of the boundary layer. The two-dimensional model also can compute wave motion near an inversion, which a 1-D model cannot. As a result, Teske and Lewellen found the temperature variance near the inversion computed with the two-dimensional model to be about twice that found with a 1-D model. This may be a unique result and should not be used for generalizing about the advantages of dimension.

33

One further practical consideration enters the picture when discussing the utility of 1-D vs. multidimensional models. In the marine environment, one rarely has the type of high resolution data necessary to provide initial and boundary conditions to a multidimensional MPBL model. Typically, only isolated radiosonde and bulk air-sea ship data area available. Such a sparse data base is more compatible with the initial and boundary condition requirements of a 1-D model. Only further study will provide answers concerning the relative merits of 1-D vs. multidimensional models.

## 3.4 OBSERVATIONS AND VERIFICATIONS

A numerical model can aid in our understanding of structure parameter profiles. But observational data must be continually used as a touchstone. Idealized model computations can have an elegant simplicity and beauty that fades when real data problems must be addressed. Observations provide the only means whereby a numerical model can be improved and validated.

Measurements of structure parameters in the marine environment are limited. The Cooperative Experiment in West Coast Oceanography and Meteorology (CEWCOM) contains a set of aircraft $C_T^2$ measurements in conjunction with bulk air-sea values. Such measurement programs remain an active area of research at the Naval Postgraduate School (Fairall et al., 1978; Davidson et al., 1978). Preliminary results from a recent field experiment off the coast of Panama City, Florida, were reported on at this workshop by Dr. Fairall. This data, and that from other large research experiments such as AMTEX and GATE, need to be exploited more fully both for model validation purposes and for the purpose of testing scaling laws.

Care must be exercised when aircraft structure parameter measurements are compared with closure model results or with scaling law predictions. Scaling laws and closure models deal, in principle, with ensemble-averaged turbulence statistics. As we know, however, ensemble averaging is hardly practical in geophysical flows, and instead one generally averages atmospheric measurements over time. The prime question then is: what averaging time of aircraft data is necessary to obtain statistics which are relevant to the predictions of the models or the scaling laws?

34

The standard two-pronged temperature probe measurements of $C_T^2$ generally require about 30 minute averages to obtain stable statistics when the measurements are made from a stationary platform. If the instrument is attached to an aircraft, about an order of magnitude advantage in averaging time can be obtained. Thus, a 3 minute average at each flight level corresponds in accuracy to the 30 minute average from a stationary platform. Shorter time averaging of the aircraft data will yield $C_T^2$ profiles having a very jagged appearance. These short-time averaged profiles cannot be directly related to scaling law or closure model results.

## 3.5 RECOMMENDATIONS - UPPER MPBL $C_n^2$ ASSESSMENT

### a. Verify 1-D Closure Model with Existing Data

The first step towards understanding $C_n^2$ in the upper MPBL by means of a numerical model must involve real data verification of the model. The existing volume of data must be searched for those cases in which sufficient information is available to supply the initial and boundary condition requirements of the model. Then comparison tests of model predictions and measured structure parameter profiles can be made. Preliminary work along these lines is reported by Burk (1978). These efforts are continuing.

Primarily for reasons of computational economy, a 1-D second-moment closure model is recommended for this numerical model study. When possible, comparison between 1-D and multidimensional model results is recommended. Comparisons among different versions of 1-D closure models are also desirable. Particular attention should be paid to improving, where possible, the closure assumptions which are used in these models.

### b. Use Closure Models to Derive Scaling Laws

As noted previously, if scaling laws are to be useful, the functional form of the universal functions must be known. For example, in Eq. (3.2) we need to know F and in Eq. (3.5) we need to know F'. We recognize that these functions may depend on the entrainment of temperature and moisture from the atmosphere above the inversion.

35

The universal functions can be established either from observations or from mathematical modeling. The latter technique is much more flexible in that many alternatives can be studied with a single program. Hence, we recommend that a numerical model be used to help develop general scaling laws which describe $C_n^2$ in the upper MPBL.

c.    Conduct Experimental Verification

The existing data base of structure function measurements in the MPBL is small. This is particularly true when those cases are discarded that have insufficient data for initializing a numerical model. For example, many of the aircraft measurements of $C_T^2$ have no wind measurements, making estimates of turbulent shear production speculative.

The existing data base is inadequate for testing the predictions of a closure model. Further, when constructing generalized scaling laws of the upper MPBL, new measurements are needed. Therefore, a new detailed field experiment is recommended. This field experiment is to be limited in scope. The preliminary scaling law and numerical model studies will define and dictate the scope of the new field experiment.

36

# REFERENCES

Badgley, F.I., C.A. Paulson, and M. Miyake, 1972: <u>Profiles of wind, temperature, and humidity over the Arabian Sea</u>. The University of Hawaii Press, 62 pp.

Burk, S.D., 1978: <u>Use of a second-moment turbulence closure model for computation of refractive index structure coefficients</u>. NAVENVPREDRSCHFAC Tech. Report TR 78-04, 58 pp.

Businger, J.A., J.C. Wyngaard, Y. Izumi, and E.F. Bradley, 1971: Flux profile relationships in the atmospheric surface layer. <u>J. Atmos. Sci</u>., 22, 181-189.

Davidson, K.L., T.M. Houlihan, C.W. Fairall, and G.E. Schacher, 1978: <u>Observations of the temperature structure function parameter, $C_T^2$, over the ocean</u>. Naval Postgraduate School Tech. Report NPS63-78-005, 37 pp.

Deardorff, J.W., 1974: Three-dimensional numerical study of turbulence in an entraining mixed layer. <u>Bound-Layer Meteor</u>., 7, 199-226.

Deardorff, J.W., 1973: Three-dimensional numerical modeling of the planetary boundary layer. <u>Workshop on Micrometeorology</u>, Amer. Meteor. Soc., 271-311.

Fairall, C.W., G.E. Schacher, K.L. Davidson, and T.M. Houlihan, 1978: <u>Atmospheric marine boundary layer measurements in the vicinity of San Nicolas Island during CEWCOM78</u>. Naval Postgraduate School Tech. Report NPS61-78-007, 70 pp.

Friehe, C., 1977: Estimation of the refractive index temperature structure parameter over the ocean. <u>Appl. Optics</u>, 10, 334-340.

Frisch, A.S., and G.R. Ochs, 1975: A note on the behavior of the temperature structure parameter in a convective layer capped by a marine inversion. <u>Jour. Appl. Meteor</u>., 14, 415-419.

Liu, W.T., 1978: The molecular effects on air-sea exchanges. Ph.D. Thesis, University of Washington, Seattle, Seattle, WA.

Sommeria, G., 1976: Three-dimensional simulation of turbulent processes in an undisturbed trade wind boundary layer. <u>Jour. Atmos. Sci</u>., 33, 216-241.

Teske, M.E., and W.S. Lewellen, 1979: Horizontal roll vortices in the planetary boundary layer. <u>Proc. Fourth Symposium on Turbulence, Diffusion and Air Pollution</u>, Amer. Meteor. Soc., 456-463.

Wesely, M.L., 1976: The combined effect of temperature and humidity fluctuations on refractive index. J. Appl. Meteor., 15, 43-49.

Wyngaard, J.C., Y. Izumi, and S. Allollis, Jr., 1971: Behavior of the refractive index structure parameter near the ground. J. Opt. Soc. Am., 61, 1646-1650.

Wyngaard, J.C., and S.F. Clifford, 1978: Estimating momentum, heat, and moisture fluxes from structure parameters. J. Atmos. Sci., 35, 1204-1211.

# APPENDIX A

## TURBULENCE ADVISORY GROUP

| | |
|---|---|
| Prof. J. Businger | University of Washington |
| Prof. C. Fairall | Naval Postgraduate School |
| Dr. C. Friehe | National Center for Atmospheric Research |
| Dr. W.S. Lewellen | Aeronautical Research Associates of Princeton |
| Prof. H. Panofsky | Penn State University |
| Prof. K. Davidson | Naval Postgraduate School |
| Dr. M. Wesely | Argonne National Laboratories |
| Prof. J. Wyngaard | CIRES, University of Colorado |
| LCDR M. Hughes | PM-22/PMS-405, Washington, DC |
| Dr. S. Burk | Naval Environmental Prediction Research Facility |
| Dr. A. Goroch | |
| Mr. P. Lowe | |
| Dr. A. Weinstein | |

# NAVY HIGH ENERGY LASER PROGRAM
## $C_n^2$ MODEL REVIEW 30 JAN 1979

## AGENDA

0900    I.  Introduction

        A. Welcoming remarks     - CAPT P. Petit (NEPRF)
        B. Introductions        - Dr. A. Weinstein (NEPRF)
        C. Goals of meeting      - Dr. A. Weinstein (NEPRF)
        D. Administrative details - Dr. A. Goroch (NEPRF)

0930    II.  HEL Program             LCDR Hughes (PMS 405)

        A. Background and plans
        B. $C_n^2$ models
           1. Model applications
           2. Requirements

1000          Discussion

1015          BREAK

1030    III.  Baseline $C_n^2$ Model     Dr. A. Goroch (NEPRF)

        A. Description

           1. Model
           2. Constants
           3. Use of $C_T^2$, $C_{Tq}^2$, $C_q^2$
           4. Natural variability from ensemble mean

1050          Discussion

1100          B. Climatology         Dr. F. Gebhardt (SAI)

1115          Discussion

1130          LUNCH

| 1300 | IV. | Model Review | Mr. P. Lowe |
|------|-----|--------------|-------------|

1300      A. Bulk meteorology, flux profile relations     Dr. J. Businger

1320      Discussion

     B. Flux parameter, $C_n^2$ relations

1330      1. Parameterization of $C_T^2$ $C_q^2$, $C_{Tq}^2$     Dr. C. Friehe

1350      2. Relating $C_n^2$ to $C_T^2$, $C_q^2$, $C_{Tq}^2$     Dr. M. Wesely

1350      Discussion

1410      C. Surface effects     Dr. J. Businger

     1. Wave effects
     2. Skin temperature effects

     Discussion

1440      BREAK

1500    V. Vertical Profiles of $C_n^2$     Dr. S. Burk

1500      A. Overview on closure models     Dr. J. Wyngaard

1520      1. 1D vs 2D models     Dr. W.S. Lewellen

1540      2. 1D model calculation sensitivity     Dr. S. Burk

1600      B. Empirical scaling laws     Dr. H. Panofsky

1620      1. Observations of vertical profiles over the ocean     Dr. C. Fairall

1640      Discussion

1700      ADJOURN

# AGENDA

## 31 JAN 1979

| | | | |
|---|---|---|---|
| 0830 | VI. | Model Adequacy Discussion | Mr. P. Lowe |

    A.   Formulation (KEYPS; Businger-Dyer)

    B.   Constants ($\gamma_n$, $\gamma_m$)

    C.   Resulting model of $C_n^2$

        1.  Model uncertainty
        2.  Natural variability

1000            BREAK

1015    VII.  Surface Effects Improvement     Dr. A. Goroch

    A.   Possible improvement with present data base

    B.   Requirements and benefits of added observations

1130            LUNCH

1300   VIII.  Vertical Extension         Dr. S. Burk

    A.   Possible improvement of present models

    B.   Requirements/benefits of added measurements

1530    IX.  Wrap Up                Dr. A. Weinstein

    A.   Meeting of original goals

    B.   Future direction

1630            ADJOURN

# APPENDIX C

## PRELIMINARY TURBULENCE MODEL

The main atmospheric effects on an optical signal are
absorption and scattering by molecules and aerosols and degrada-
tion of the signal by atmospheric turbulence. The following
presents a preliminary model of the intensity of atmospheric
turbulence as a function of bulk meteorological variables. This
model is currently used by the Navy HEL program. At this point,
however, the model is to serve as a start of discussion with all
segments open to modification.

The effect of refractive index inhomogeneities on a coherent
laser beam is to focus a segment of the beam to a point determined
by the size and location of the inhomogeneity. Over a long path
this causes a defocusing and loss of coherence in the beam. An
analysis of turbulent effects on beam characteristics requires
assessment of a mean value of the intensity of turbulence over
the beam path, and for the time of transmission.

## Calculation of Optical Parameters

The inhomogeneities of index of refraction are described by
an index of refraction structure constant $C_n^2$, defined as

$$C_n^2 = \frac{1}{[n(r_1)-n(r_2)]^2} (|r_1-r_2|)^{-2/3} \qquad (1)$$

The optical index of refraction of air is related to tempera-
ture T and water vapor pressure e,

$$n = 1 + A_1 \frac{p-e}{T} + A_2 \frac{e}{T} \qquad (2)$$

where $A_1$ and $A_2$ are constants.

The fluctuation of refractive index are therefore related to
fluctuations of temperature and humidity and their correlation
(Wesely, 1973),

$$C_n^2 = B_1\frac{P^2}{T^4}C_T^2 + B_2\frac{P^2}{T^3}C_{eT}^2 + B_3\frac{1}{T^2}C_e^2 \tag{3}$$

where $B_1$, $B_2$, and $B_3$ are constants.

The first term is dominant in dry conditions. The second term can contribute significantly under special humidity conditions described by Friehe (1977). The preliminary model neglects the latter two contributions for two reasons. First, the $C_T^2$ contribution is the dominant conttribution to the refractive index structure function. Second, there are no preliminary parameterizations of $C_{eT}^2$ and $C_T^2$ available which have been verified as extensively as those of $C_T^2$ (Wesely, 1973; Friehe, 1977).

By a combination of dimensional arguments and curve fitting to the Kansas data base, Wyngaard et al. (1971) derived a semi-empirical relationship of $C_T^2$ and turbulence parameters.

$$C_T^2 = T_*^2 \, Z^{-2/3} g(Z_a/L) \tag{4}$$

where

$$g(Z_a/L) = \begin{cases} 4.9(1-7\,Z_a/L)^{-2/3} & Z_a/L \le 0 \\ 4.9(1+2.75\,Z_a/L) & Z_a/L \ge 0 \end{cases}$$

This parameterization seems to also be valid over the ocean, if proper experimental precautions are taken during the measurement (Friehe, 1977).

## Calculation of Turbulence Parameters

The turbulence parameters $T_*$ and $L$ are calculated from the bulk meteorological variables using semi-empirical heat and momentum flux profiles. Two commonly used formulations of these profiles are the KEYPS (Lumley and Panofsky, 1964) and the Businger-Dyer formulas (Businger et al., 1971). The Businger-Dyer formalism was chosen to represent the flux profiles because it is widely used and is part of the approximation formulas to be described below.

The calculation of the height by the Monin-Obukhov length $Z_a/L$ proceeds with the approximation used by Barker and Baxter (1975). The scaled height is given by

$$\frac{Z_a}{L} = \left[\frac{2gZ_a(T_{va}-T_{vo})}{U_a^2(T_{va}+T_{vo})}\right] \frac{[\ln(Z_a/Z_0) + \psi_m(z_a/L)]^2}{R[\ln(Z_a/Z_0)+\psi_H(Z_a/L)]} \tag{5}$$

where (for unstable conditions)

$$\psi_m = -\ln\left[\left(\frac{1+\varepsilon^2}{2}\right)\left(\frac{1+\varepsilon}{2}\right)^2\right] + 2 \arctan(\varepsilon) \quad \frac{\pi}{2}$$

$$\varepsilon = [1-\gamma_m Z_a/L]^{1/4}$$

$$\psi_H = -2\ln\left[\frac{1}{2}(1 + \sqrt{1-\gamma_H Z_a/L})\right]$$

Using the definition of bulk Richardson number

$$R_i = \frac{2gZ_a}{V_a^2} \frac{T_{va}-T_{vo}}{T_{va}+T_{vo}} \tag{6}$$

Barker and Baxter find an approximate form for $\frac{Z_a}{L}$,

$$\frac{Z_a}{L} = R_i\left[0.471\frac{1}{k}\ln\left(\frac{Z_a}{Z_0}\right) - 1.045\right] \tag{7}$$

This equation is inaccurate for $0 \le \frac{Z_a}{L} \le -0.05$ in which case one uses

$$\frac{Z_a}{L} = \ln\left(\frac{Z_a}{Z_0}\right) \left\{ \frac{R_i - \frac{R}{2\beta} + \sqrt{\frac{1-R}{\beta}R_i + \frac{R^2}{4\beta^2}}}{1-\beta R_i} \right\} \tag{8}$$

The temperature function $T_*$ is obtained from an integration of the flux profile relationships

47

$$T_* = \frac{k(T_a - T_s)}{R[\ln(\frac{Z_a}{Z_o}) + \psi_H]} \qquad (9)$$

The several constants in the flux profile relationships have a range of values attributed to them in the literature. Yaglom (1974) points out that the momentum profile constant $\gamma_m$ is accepted at about 15 or 16 by several authors. The heat profile constant, $\gamma_H$, however, has been given a range of values from 9 (Businger et al., 1971) from the Kansas data to 18 over the Utah desert (Monji, 1973).

Laboratory measurements of the von Karmann constant k range from 0.2 to 0.8, although atmospheric measurements show values from 0.3 to 0.44. The roughness length over the ocean is generally determined from Charnock's (1955) relation

$$Z_o = \alpha \frac{U_*^2}{g} \qquad (10)$$

where $\alpha$ ranges from 0.077 (Roll, 1965) to 0.0144 (Garrett, 1977).

In choosing the values of the constants for this model, it was realized that there is an interdependence among them during most measurement programs. Hence we chose a set of constants consistent with one experimental set of data. Since the Kansas data is widely accepted as a careful and extensive set of measurements, the constants developed by Businger et al. (1971) are being used. These are

$$k = 0.35, \quad \gamma_m = 16, \quad \gamma_H = 9$$

Because of the uncertainty in the calculation of $Z_o$, a constant value of $4 \times 10^{-4}$ m was chosen, independent of wind speed. This is at least consistent with marine measurements of Badgley et al. (1972).

# GLOSSARY FOR PRELIMINARY TURBULENCE MODEL

$C_T^2$    - Temperature structure function

$C_n^2$    - Index of refraction structure function

$C_e^2$    - Water vapor density structure function

$C_{eT}^2$ - Coefficient of cospectrum of water vapor and temperature

$e(T)$ - Vapor pressure at temperature T (mb)

$g$      - 9.8 m sec$^{-2}$ force of gravity

$k$      - .35, von Karmann constant

$L$      - Monin-Obukhov length (m)

$n$      - Optical index of refraction

$P$      - Air pressure (mb)

$q$      - Vapor density

$RH$    - Relative humidity at height Z, (%)

$Ri$    - Bulk Richardson number

$R$      - .74

$T$      - Temperature (K)

$T_a$    - Temperature at height Z

$T_s$    - Sea surface temperature

$T_v$    - Virtual temperature (°K)

$T_{va}$   - Virtual temperature at height Z

$T_{vs}$   - Virtual temperature at sea surface

$T_*$    - Friction temperature

$U_a$    - Wind speed at height $Z_a$ (usually Z = 10 m) (m sec$^{-1}$)

$U_*$    - Friction speed

$Z_a$    - Height (m)

49

$Z_o$   - Roughness length (m)

$\alpha$   - Roughness length constant

$\beta$   - 4.7 constant of Barker & Baxter (1975)

$\gamma_H$   - Heat flux profile parameter

$\gamma_m$   - Momentum flux profile parameter

50

# REFERENCES FOR PRELIMINARY TURBULENCE

Badgley, F.I., C.A. Paulson, and M. Miyake (1972)
Profiles of wind temperature, and humidity over the Arabian Sea.
The University of Hawaii Press.

Barker, E. H. and T. L. Baxter (1975)
A note on the computation of atmospheric surface layer fluxes
for use in numerical modeling.
J. Appl. Meteor. $\underline{14}$ (4), 620-622.

Businger, J. A., J. C. Wyngaard, Y. Izumi, and E. F. Bradley (1971)
Flux profile relationships in the atmospheric surface layer.
J. Atmos. Sci., $\underline{22}$, 181-189.

Charnock, H. (1955)
Wind stress on a water surface.
Quart. J. Roy. Meteorol. Soc., $\underline{81}$, 639-640.

Davidson, K. L., T. M. Houlihan, C. W. Fairall, and G. E. Schacher
(1978)
Observations of the temperature structure function parameter, $C_T^2$,
over the ocean.
To be published.

Friehe, C. (1977)
Estimation of the refractive index temperature structure parameter
over the ocean.
Appl. Optics, $\underline{10}$, 334-340.

Garratt, J. R. (1977)
Review of drag coefficients over oceans and continents.
Mon. Wea. Rev. $\underline{105}$, 915-929.

Lumley, J. L. and H. A. Panofsky (1964)
The structure of atmospheric turbulence.
Interscience Publ.

Monji, N. (1973)
Budgets of turbulent energy and temperature variance in the
transition zone from forced to free convection.
J. Meteor. Soc. Japan, Ser. II, $\underline{51}$ (2), 133-145.

Roll, H. U. (1965)
Physics of the marine atmosphere.
Academic Press.

Wesely, M. L. (1976)
The combined effect of temperature and humidity fluctuations on
refractive index.
J. Appl. Meteor., $\underline{15}$, 43-49.

Wyngaard, J. C., Y. Izumi, and S. Allollis, Jr. (1971)
Behavior of the refractive index structure parameter near the
ground.
J. Opt. Soc. Am., 61, (12), 1646-1650.

Wyngaard, J. C. and S. F. Clifford (1978)
Estimating momentum, heat, and moisture fluxes from structure
parameters.
J. Atmos. Sci., 35, 1204-1211.

Yaglom, A. M. (1974)
Data on turbulence characteristics in the atmospheric surface
layer.
Izv. Atm. Ocean. Physi., 10 (6), 566-586.

# APPENDIX D

## Humidity Effects in $C_n^2$ within the Surface Layer

by

### H. A. Panofsky

We begin by defining $N_*$, by analogy to $T_*$,

$$N^* = - \frac{\overline{w'n'}}{U_*} \tag{D.1}$$

where n' represents fluctuations of refractive index and remaining terms are defined in the body of the report. For the optical wavelength, n' is related to temperature T' and humidity q' fluctuations by (Friehe, 1977)

$$n' = (K_1 T' + K_2 \rho q') \times 10^{-6} \tag{D.2}$$

where $K_1 = -1.0\,°K^{-1}$ and $K_2 = -.05667\ cm^3/microgram$. The air density, $\rho$, is taken to be $1.25 \times 10^{-3}\ gm\ cm^{-3}$.

Multiplying (D.2) by w' and dividing by $U_*$, we get

$$N_* = - (T_* + 71Q_*) \times 10^{-6} \tag{D.3}$$

$$= - T_*(1 + \frac{.03}{B})$$

Next we introduce Monin-Obukhov scaling with the scaling function $N_*$ for index fluctuations. Then, proceeding as with $C_T^2$, we get

$$C_n^2 = N_*^2\ Z^{-2/3}\ G(z/L) \tag{D.4}$$

If the universal functions for q and T are equal to each other (as they seem to be over land) G(z/L) should equal g(z/L). This can be seen more exactly if dissipation of refractive index fluctuations is in balance with the production of these fluctuations. Hence we finally have

53

$$c_n^2 = (K_3)^2 \, c_T^2 \left(1 + \frac{.03}{B}\right)^2$$

where $K_3 = 10^{-6} \, P/T^2$. This is identical to the result of Wesely (1976) when temperature and moisture are taken to be perfectly correlated.